



Evidence for atmospheric variability over the Pacific on decadal timescales

R. J. Burgman,¹ A. C. Clement,¹ C. M. Mitas,¹ J. Chen,² and K. Esslinger¹

Received 27 August 2007; revised 30 October 2007; accepted 8 November 2007; published 4 January 2008.

[1] An index of Pacific decadal variability based on a multivariate empirical orthogonal function analysis of National Centers for Environmental Prediction reanalysis is used to extract associated signals in satellite-based measurements of atmospheric parameters. This index captures the 1976–1977 “El Niño–Southern Oscillation (ENSO)-like” warming shift of sea surface temperatures (SST) as well as a more recent transition of opposite sign in the 1990s. Utilizing measurements of water vapor, wind speed, precipitation, long-wave radiation, as well as surface observations, our analysis shows evidence of the atmospheric changes in the mid-1990s that accompanied the “ENSO-like” interdecadal SST changes. **Citation:** Burgman, R. J., A. C. Clement, C. M. Mitas, J. Chen, and K. Esslinger (2008), Evidence for atmospheric variability over the Pacific on decadal timescales, *Geophys. Res. Lett.*, 35, L01704, doi:10.1029/2007GL031830.

1. Introduction

[2] Pacific decadal variability (PDV) and its possible impacts on regional and global climate has been the subject of much research in recent years [Mantua *et al.*, 1997; Deser *et al.*, 2004; Seager *et al.*, 2005]. The sea surface temperature (SST) structure of PDV is well known and is characterized by a broad triangular pattern in the tropical Pacific surrounded by opposite anomalies in the mid-latitudes of the central and western Pacific Basin. Studies of century long reconstructions of SST and sea level pressure (SLP) suggest several “regime shifts” have occurred during the 20th century [Zhang *et al.*, 1997; Deser *et al.*, 2004]. While several potential mechanisms for these low-frequency changes in the tropical Pacific have been suggested [Kleeman *et al.*, 1999; Barnett *et al.*, 1999; Hazeleger *et al.*, 2005; Schopf and Burgman, 2006; Burgman, 2006], the cause of PDV remains unclear.

[3] One issue that has contributed to the debate over the mechanism behind PDV is the lack of data covering the periods of these transitions. Prior studies have relied primarily on SST and SLP data to characterize PDV, though more recently Deser *et al.* [2004] have shown consistent patterns in precipitation and cloud cover. In this study, we add to the picture of PDV by including decades-long satellite observations which have complete spatial coverage over the Pacific, and which provide information about

atmospheric quantities not previously studied in association with PDV.

[4] The literature suggests that in addition to the 1976 shift, another climate transition occurred in the mid 1990s [Peterson and Schwing, 2003; Chen *et al.*, 2007b]. These changes coincide with observed decadal-scale changes in the tropical mean radiation balance [Wielicki *et al.*, 2002; Wong *et al.*, 2006; Chen *et al.*, 2002]. There is also evidence for changes in the atmospheric circulation over this period. Vecchi *et al.* [2006] and Zhang and Song [2006] show that while the Walker circulation has weakened over the past century, there is an increase in strength during the 1990s. Hoerling and Kumar [2003] show that subtropical subsidence was stronger after the 1990s than in prior decades. In this study, we examine the spatial patterns of decadal variability in the atmosphere using recently revised satellite products, with a focus on the period 1988–2003 for the tropical and subtropical Pacific.

2. Data

[5] The data sets used in this study include the following: (1) National Centers for Environmental Prediction (NCEP)/National Center for Atmospheric Research (NCAR) reanalysis surface temperature, zonal wind, meridional wind, vertical velocity, and specific humidity (1948–2006) [Kalnay *et al.*, 1996], (2) Special Sensor Microwave Imager (SSM/I) V6 wind speed and water vapor from Remote Sensing Systems (1987–2006), (3) High Resolution Infrared Radiation Sounder (HIRS) outgoing longwave radiation (OLR) (1979–2003) [Lee *et al.*, 2004], (4) NOAA Extended Reconstructed SST data (ERSST.v2) provided by the NOAA CIRES Climate Diagnostics Center, Boulder, Colorado, USA, from their Web site at <http://www.cdc.noaa.gov/> (1854–2004) [Smith and Reynolds, 2004], (5) Global Precipitation Climatology Project (GPCP) monthly precipitation analysis (1979–Present) [Adler *et al.*, 2003], and (6) ICOADS release 2.1 cloud amount (1800–2005) [Worley *et al.*, 2005].

3. Analysis

[6] In order to construct an index for PDV, we follow the procedure of Chen *et al.* [2007a]. Those authors use five NCEP/NCAR reanalysis variables (air temperature, zonal wind, meridional wind, vertical velocity, and specific humidity) for the lowest 8 pressure levels (1000 hPa–300 hPa) in the 60°S–60°N region over the time period 1970 to 2003. The El Niño–Southern Oscillation (ENSO) signal is “removed” from these data using the extreme cross-correlations at the least lag (ECLL) of the 6-yr high-pass NINO34 index with each climate variable [Chen *et al.*, 2007a]. The

¹Rosenstiel School for Marine and Atmospheric Science, University of Miami, Miami, Florida, USA.

²Earth System Science Interdisciplinary Center, University of Maryland, College Park, Maryland, USA.

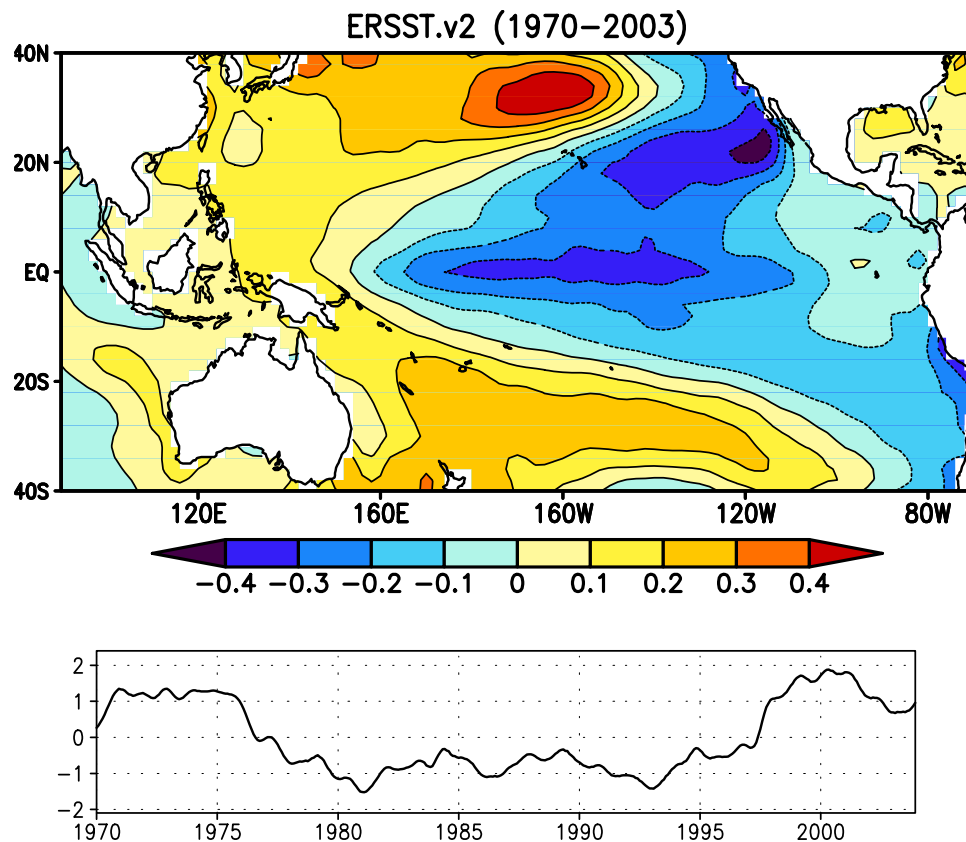


Figure 1. The second (normalized) PC time series of the PDV mode of the 1970–2003 “ENSO-removed” NCEP combined EOF analysis and associated regression pattern for SST [*Chen et al.*, 2007b].

removal procedure is only applied to grid boxes where ECLL is statistically confident above the 99% level. We note that while persistence of the ENSO signal as well as nonlinearity and asymmetry play a role [*Power and Colman*, 2006; *Trenberth et al.*, 1998; *Schopf and Burgman*, 2006], the first order ENSO signal is captured by the linear analysis performed here.

[7] Next, empirical orthogonal function (EOF) analysis is performed on this “ENSO-removed” data set of 40 NCEP/NCAR parameters listed above (ER-NCEP40p). A 12-month running mean is applied to the data prior to the EOF analysis and comprises the only filtering of the variables in this study. The first EOF explains 16.4% of the combined variance and captures what *Chen et al.* [2007a] interpret as the global warming signal [not shown]. The second EOF explains 9.6% of the variance, and has similar spatial structure in SST as the PDV reported in previous studies [e.g., *Zhang et al.*, 1997; *Deser et al.*, 2004]. Figure 1 shows the normalized principal component (PC) of EOF2 and the associated spatial pattern of SST derived from regression analysis. Note that the ER-NCEP40p PC2 captures the 1976 climate transition as well as the more recent transition in the mid-1990s.

[8] While this procedure is somewhat different than previous ways of defining PDV (e.g., EOF 1 of north Pacific SST [*Mantua et al.*, 1997], EOF 1 of low-pass-filtered Pacific SST [*Yeh and Kirtman*, 2004], results are similar for the 1976 transition. Because the satellite data

covers a shorter period, filtering techniques used in previous studies are not appropriate for defining decadal variability over this period. The methodology we use here provides a more general index for PDV which we use to characterize the spatial structure of the PDV mode in the satellite data by regressing the grid point values of the unfiltered anomaly fields from the data sets listed above upon the normalized ER-NCEP40p PC2 time series. The spatial patterns are quite similar if we were to calculate straight linear trends for the same period (without removing ENSO), but alleviates the dependence of the trends on the end points.

[9] We refrain from referring to these regression patterns as statistically significant modes of variability due to the length of the record analyzed, though the signals in the northeast subtropical Pacific and western equatorial Pacific that are discussed in the text are statistically significant at the 95% confidence level. Also, we emphasize the signals that are physically consistent among different variables in these independent data sets. It is important to note that this analysis technique does not separate changes associated with PDV from those related to greenhouse gas forcing for the time period 1988–2003. While the time series of PC2 does not increase monotonically over this period (like greenhouse gas forcing), it is dominated by a trend which is primarily due to the ’90s shift. Hence, our focus is on the regional structure of the regression results, which we argue is strongly influenced by PDV, and the similarity of the

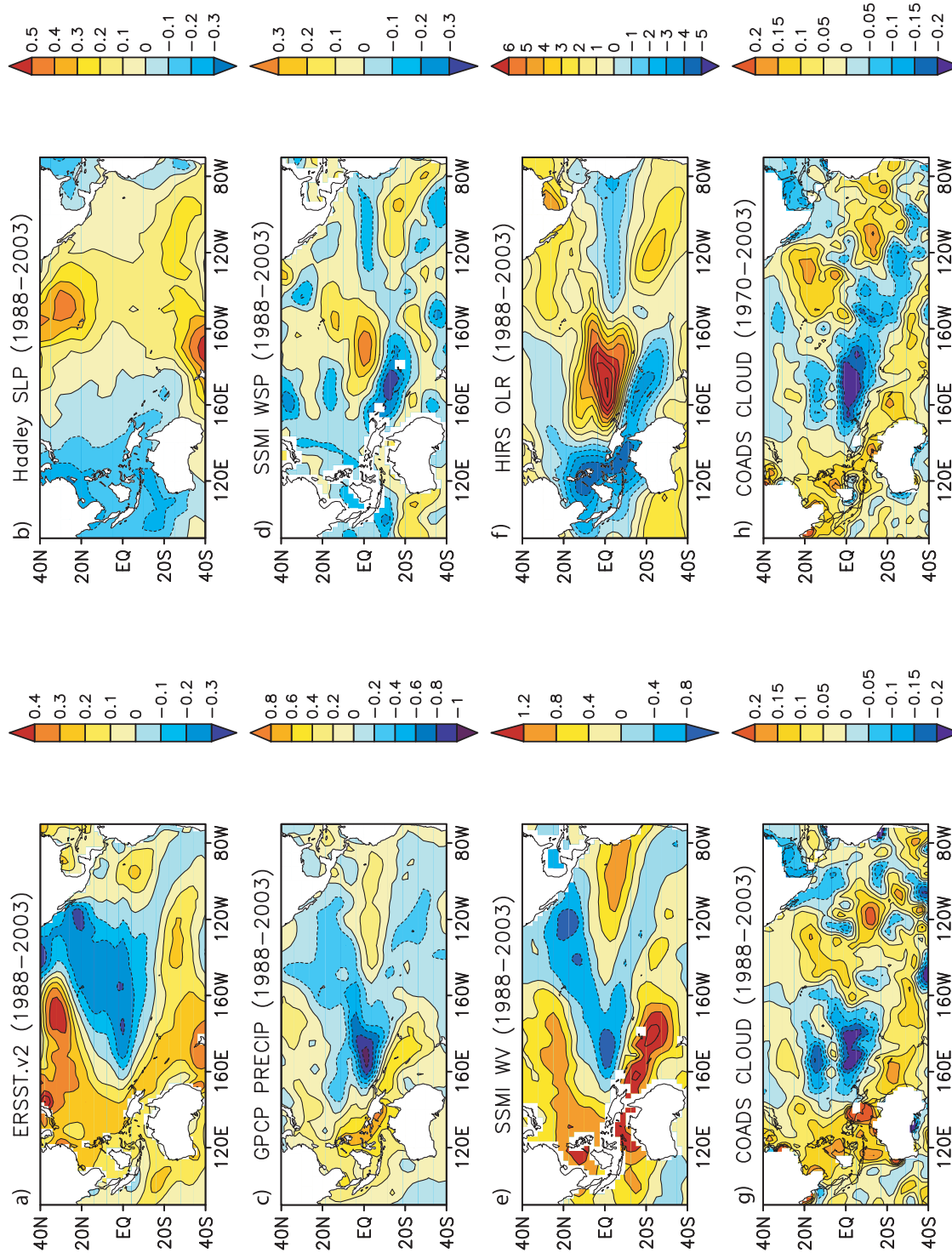


Figure 2. Spatial patterns generated by regressing the global (a) SST field upon the timeseries shown in Figure 1. Contour interval $0.1^{\circ}\text{C} (\text{STDV})^{-1}$. (b) As in Figure 2a for SLP. Contour interval $0.1\text{mb} (\text{STDV})^{-1}$. (c) GPCP precipitation. Contour interval $0.2 \text{mm/day} (\text{STDV})^{-1}$. (d) SSM/I wind speed. Contour interval $0.1\text{ms}^{-1} (\text{STDV})^{-1}$. (e) SSM/I atmospheric WV. Contour interval $0.4\text{mm} (\text{STDV})^{-1}$. (f) HIRS outgoing longwave radiation. Contour interval $1\text{Wm}^{-2} (\text{STDV})^{-1}$. (g) ICOADS cloud amount. Contour interval $0.05 \text{octas} (\text{STDV})^{-1}$. (h) As in Figure 2g for period January 1970 to December 2003.

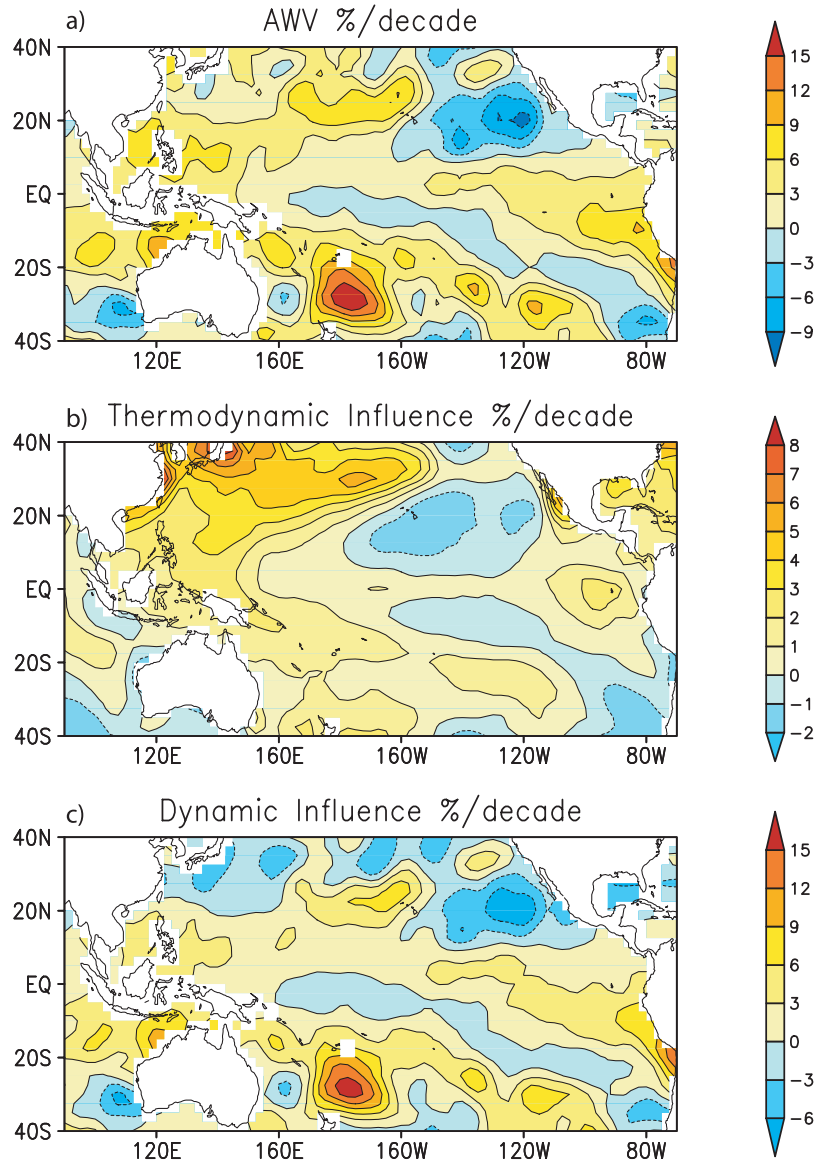


Figure 3. (a) Fractional change of AWV associated with mid 1990s transition (as in Figure 2e). Contour interval $3\%(\text{decade})^{-1}$. (b) Thermodynamic influence. Contour interval $1\%(\text{decade})^{-1}$. (c) Dynamic influence. Contour interval $3\%(\text{decade})^{-1}$.

spatial structure to previous transitions (e.g., Figures 1 and 2) supports this contention.

4. Results

[10] The spatial signature of the low-frequency variability in different quantities associated with the normalized ER-NCEP40p PC2 time series is shown in Figures 2a–2f. The period of the study, 1988 through 2003, is chosen as it is the period of coverage common to all of the data sets. The contours on the maps have the same dimensions as the fields themselves, and their numerical values are indicative of the anomalies associated with typical (i.e., unit standard deviation) amplitudes of the PC time series (as by *Zhang et al.* [1997]). The SST pattern (Figure 2a) is characterized by the same “ENSO-like” pattern shown in previous studies. Despite the large 1997–98 El Niño event, both this analysis as well as a linear trend show a cooling in

the eastern Pacific basin, or a “La Niña-like” SST change, over this period. We note that in previous transitions, the SST signals in the subtropics were fairly symmetric north and south of the equator, while during the 1990s transition, the signal is larger in the northern subtropics.

[11] SLP is shown in Figure 2b. Again, the well-known PDV structures appears, with an increase in the east-west SLP gradient on the equator and large signals in the north Pacific. The increased SLP in the north Pacific, which represents a weakening of the Aleutian low, extends into the eastern subtropics where it constitutes an increase in the climatological high pressure there. Figure 2c shows that precipitation shifts westward on the equator, consistent with the changes in SST and SLP gradients. Deep convection in the western tropical Pacific comprises the rising branch of the vertical atmospheric circulation in the Pacific basin and an increase in precipitation here suggests a strengthening of

the general atmospheric circulation in the tropical Pacific. The increase in SLP in the subtropics where the descending branch of the circulation occurs is also consistent with an increase in the meridional overturning circulation in the Pacific over the period [Zhang and Song, 2006].

[12] Figure 2d shows the wind speed pattern associated with EOF 2. In the equatorial Pacific there is an increase in wind speed centered at 170°W collocated with the changes in SST and SLP gradient, which implies an increase in the trade wind strength and Walker circulation associated with the “La Niña-like” phase of the PDV. In the northeastern subtropics the signal is small and negative over the region of the large amplitude negative SST signal. This suggests that the cooling in this region is not due to an increase in the turbulent heat fluxes.

[13] Figure 2e shows the linear regression coefficients between the normalized ER-NCEP40p PC2 time series and SSM/I atmospheric water vapor (WV). This pattern is actually quite different in spatial structure from the pattern that occurs on interannual timescales associated with ENSO [Trenberth *et al.*, 2005] because of its broad meridional scale. At first glance one might assume the decadal changes in WV are simply thermodynamically forced by changes in the SST's seen in Figure 2a, which would predict a uniform 6.4% increase in WV per degree change in SST [Stephens, 1990; Held and Soden, 2006]. We use this relation to remove the WV change attributable to SST in order to identify changes due to large scale circulation [Blankenship and Wilheit, 2001]. Figure 3a shows the fractional change in the “ENSO-removed” WV trend over the 1988–2003 period. To find the thermodynamic contribution to the change in WV, we scale the “ENSO-removed” SST trend over the same period by 6.4% (Figure 3b). The difference between the total and thermodynamic components is shown in Figure 3c, and represents the possible influence of dynamics on the WV distribution. The significant drying over the eastern subtropical oceans over this period clearly can not be explained by thermodynamics alone [Hoerling and Kumar, 2003; Esslinger, 2006]. A regression of PC2 on ERA40 and NCEP Reanalysis 2 vertical velocity fields [Chen *et al.*, 2007b] support these results though the reliability of these data is questionable [Kinter *et al.*, 2004; Mitas and Clement, 2006].

[14] Figure 2f shows the regression coefficients between the normalized PDV index and HIRS OLR. In the tropics, a westward shift in convection in the western Pacific results in decreasing OLR over Indonesia with a large increase at 170°E on the equator. These changes are likely due to changes in high clouds associated with deep convection, and are consistent with the precipitation changes (Figure 2c). In the subtropics the increase in OLR coincides with decreased SST and a decrease in WV. Together, this suggests that the increased radiation to space is related to drying which may be due to atmospheric circulation changes. A similar analysis using OLR from the Earth Radiation Budget Experiment [not shown] is in agreement with the pattern seen here. Again, this subtropical signal does not appear on interannual timescales associated with ENSO where the signal is mainly confined to the equator [Wong *et al.*, 2000].

[15] Figure 2g shows the relationship between surface observations of cloudiness from ICOADS and the ER-NCEP40p PC2 time series. In the western Pacific the

change in cloudiness is consistent with changes in convection as seen in the OLR and precipitation. There is a slight increase in cloud cover in parts of the stratus regions of the eastern tropics coinciding with regions of SST cooling, drying and high OLR. Analysis of ICOADS clouds for the period 1970–2003 (Figure 2h) show a more symmetric pattern of cloudiness in the eastern subtropics with larger amplitude for the previous transition. There is some support for this increase in subtropical cloudiness since the mid 1980s from a trend analysis of a corrected version of the International Satellite Cloud Climatology Project data set (J. Norris, personal communication, 2007). Stratus clouds play an important role in the radiation budget in the subtropics due to their relatively high albedo. An increase in cloud amount in the subtropics increases the albedo, reducing the amount of solar radiation that reaches the surface, which could indicate a possible feedback between the boundary layer and the underlying SST.

5. Summary and Conclusions

[16] While PDV has been extensively studied in surface-based observations such as SST and SLP, little is known about the role of the atmosphere in such variability. Here we present changes in surface winds, WV, OLR, and clouds occurring on decadal timescales in the central equatorial Pacific and eastern subtropics. The most recent climate shift, which occurred in the 1990s during a period of continuous satellite coverage, is characterized by a “La Niña-like” SST pattern with significant signals in the central equatorial Pacific and also in the northeastern subtropics. There is a clear westward shift in convection on the equator, and an apparent strengthening of the Walker circulation. In the north-eastern subtropics, SST cooling coinciding with atmospheric drying appears to be induced by changes in atmospheric circulation. There is no indication in the wind speed that the changes in SST or WV are a result of changes in the surface heat flux. There is also an increase in OLR which is consistent with the drying. Finally, there is evidence for an increase in cloud fraction in the stratus regions for the 1990s transition as seen in earlier studies. Together, these results suggest that there are decadal-scale changes in the atmosphere involving circulation, water vapor, clouds and radiation that may play a role in PDV, and are worthy of further study.

[17] **Acknowledgments.** The authors would like to thank J. Norris for informative discussions of the COADS cloud data. We are also grateful for discussions with N. Mantua, B. Kirtman, and P. Zuidema. R. B. and A. C. were funded by NASA grant NNG04GM67G and NOAA grant NA060AR4310142.

References

- Adler, R. F., *et al.* (2003), The Version 2 Global Precipitation Climatology Project (GPCP) monthly precipitation analysis (1979–Present), *J. Hydro-meteorol.*, *4*, 1147–1167.
- Barnett, T. P., D. W. Pierce, M. Latif, D. Dommenget, and R. Saravanan (1999), Interdecadal interactions between the Tropics and midlatitudes in the Pacific basin, *Geophys. Res. Lett.*, *26*, 615–618.
- Blankenship, C. B., and T. T. Wilheit (2001), SSM/T-2 measurements of regional changes in three-dimensional water vapor fields during ENSO events, *J. Geophys. Res.*, *106*, 5239–5254.
- Burgman, R. J. (2006), Enso decadal variability, Ph. D. thesis, George Mason Univ., Fairfax, Va.
- Chen, J., B. E. Carlson, and A. D. Del Genio (2002), Evidence for strengthening of the tropical general circulation in the 1990s, *Science*, *295*, 838–841.

- Chen, J., A. D. Del Genio, B. E. Carlson, and M. G. Bosilovich (2007a), The spatiotemporal structure of 20th century climate variations in observations and reanalyses. Part I: Long-term trend, *J. Clim.*, in press.
- Chen, J., A. D. Del Genio, B. E. Carlson, and M. G. Bosilovich (2007b), The spatiotemporal structure of 20th century climate variations in observations and reanalyses. Part II: Pacific pan-decadal variability, *J. Clim.*, in press.
- Deser, C., A. S. Phillips, and J. W. Hurrell (2004), Pacific interdecadal climate variability: Linkages between the tropics and the North Pacific during boreal winter since 1900, *J. Clim.*, *17*, 3109–3124.
- Esslinger, K. (2006), An analysis of column integrated water vapor trends adjusted for ENSO, M. S., Univ. of Miami, Miami, Fla.
- Hazeleger, W., C. Severijns, R. Seager, and F. Molteni (2005), Tropical Pacific driven decadal energy transport variability, *J. Clim.*, *18*, 2037–2051.
- Held, I. M., and B. J. Soden (2006), Robust responses of the hydrological cycle to global warming, *J. Clim.*, *19*, 5686–5699.
- Hoerling, M., and A. Kumar (2003), The perfect ocean for drought, *Science*, *299*, 691–694, doi:10.1126/science.1079053.
- Kalnay, E., et al. (1996), The NCEP/NCAR 40-year reanalysis project, *Bull. Am. Meteorol. Soc.*, *77*, 437–471.
- Kinter, J. L., M. J. Fennessy, V. Krishnamurthy, and L. Marx (2004), An evaluation of the apparent interdecadal shift in the tropical divergent circulation in the NCEP-NCAR reanalysis, *J. Clim.*, *17*, 349–361.
- Kleeman, R., J. P. McCreary, and B. A. Klinger (1999), A mechanism for generating ENSO decadal variability, *Geophys. Res. Lett.*, *26*, 1743–1746.
- Lee, H. T., A. Gruber, and R. G. Ellingson (2004), HIRS outgoing longwave radiation climate data record, paper presented at CLIVAR 2004 1st International CLIVAR Science Conference, Int. CLIVAR Proj. Off., Baltimore, Md.
- Mantua, N. J., S. R. Hare, Y. Zhang, J. M. Wallace, and R. C. Francis (1997), A Pacific interdecadal climate oscillation with impacts on salmon production, *Bull. Am. Meteorol. Soc.*, *78*, 1069–1079.
- Mitas, C. M., and A. Clement (2006), Recent behavior of the Hadley Cell and tropical thermodynamics in climate models and reanalyses, *Geophys. Res. Lett.*, *33*, L01810, doi:10.1029/2005GL024406.
- Peterson, W. T., and F. B. Schwing (2003), A new climate regime in northeast Pacific ecosystems, *Geophys. Res. Lett.*, *30*(17), 1896, doi:10.1029/2003GL017528.
- Power, S., and R. Colman (2006), Multi-year predictability in a coupled general circulation model, *Clim. Dyn.*, *26*, 247–272.
- Schopf, P. S., and R. J. Burgman (2006), A simple mechanism for ENSO residuals and asymmetry, *J. Clim.*, *19*, 3167–3179.
- Seager, R., Y. Kushnir, C. Herweijer, N. Naik, and J. Velez (2005), Modeling of tropical forcing of persistent droughts and pluvials over western North America: 1856–2000, *J. Clim.*, *18*, 4065–4088.
- Smith, T. M., and R. W. Reynolds (2004), Reconstruction of monthly mean oceanic sea level pressure based on COADS and station data (1854–1997), *J. Atmos. Oceanic Technol.*, *21*, 1272–1282.
- Stephens, G. L. (1990), On the relationship between water vapor over the oceans and sea surface temperature, *J. Clim.*, *3*, 634–645.
- Trenberth, K. E., G. W. Branstator, D. Karoly, A. Kumar, N. Lau, and C. Ropelewski (1998), Progress during TOGA in understanding and modeling global teleconnections associated with tropical sea surface temperatures, *J. Geophys. Res.*, *103*, 14,291–14,324.
- Trenberth, K. E., J. Fasullo, and L. Smith (2005), Trends and variability in column-integrated atmospheric water vapor, *Clim. Dyn.*, *24*, 741–758.
- Vecchi, G. A., B. J. Soden, A. T. Wittenberg, I. M. Held, A. Leetmaa, and M. J. Harrison (2006), Weakening of tropical Pacific atmospheric circulation due to anthropogenic forcing, *Nature*, *441*, 73–76.
- Wielicki, B. A., et al. (2002), Evidence for large decadal variability in the tropical mean radiative energy budget, *Science*, *295*, 841–844.
- Wong, T., D. F. Young, M. Haeflelin, and S. Weckmann (2000), Validation of the CERES/TRMM ERBE-like monthly mean clear-sky longwave dataset and the effects of the 1998 ENSO event, *J. Clim.*, *13*, 4256–4267.
- Wong, T., B. A. Wielicki, R. B. Lee, G. L. Smith, K. A. Bush, and J. K. Willis (2006), Reexamination of the observed decadal variability of the Earth radiation budget using altitude-corrected ERBE/ERBS nonscanner WFOV data, *J. Clim.*, *19*, 4028–4040.
- Worley, S. J., S. D. Woodruff, R. W. Reynolds, S. J. Lubker, and N. Lott (2005), ICOADS release 2.1 data and products, *Int. J. Climatol.*, *25*, 823–842.
- Yeh, S.-W., and B. P. Kirtman (2004), Tropical Pacific decadal variability and ENSO amplitude modulation in a CGCM, *J. Geophys. Res.*, *109*, C11009, doi:10.1029/2004JC002442.
- Zhang, M., and H. Song (2006), Evidence of deceleration of atmospheric vertical overturning circulation over the tropical Pacific, *Geophys. Res. Lett.*, *33*, L12701, doi:10.1029/2006GL025942.
- Zhang, Y., J. M. Wallace, and D. S. Battisti (1997), ENSO-like interdecadal variability: 1900–93, *J. Clim.*, *10*, 1004–1020.

R. J. Burgman, A. C. Clement, K. Esslinger, and C. M. Mitas, MPO, RSMAS, University of Miami, 4600 Rickenbacker Causeway, Miami, FL 33149, USA. (rburgman@rsmas.miami.edu)

J. Chen, Earth System Science Interdisciplinary Center, University of Maryland, College Park, MD 20742, USA.